processes

MDPI

Article

Study on the Plugging Limit and Combination of CO_2 Displacement Flow Control System Based on Nuclear Magnetic Resonance (NMR)

Chang-Hua Yang [1,2,*], Pan-Pan Lu [1], Ya-Ming Cao [3], Min Xu [1], Zhen-Ye Yu [1] and Peng-Fei Cheng [1]

[1] School of Petroleum Engineering, Xi'an Shiyou University, Xi'an 710065, China; lupanan98@163.com (P.-P.L.); xuminn1130@163.com (M.X.); yzhenye@163.com (Z.-Y.Y.); cpf12345qwer@163.com (P.-F.C.)
[2] Engineering Research Center for Development and Treatment of Low-ultra-Low-Permeability Reservoirs in Western China, Ministry of Education, Xi'an 710065, China
[3] Drilling and Production Technology Research Institute, Jidong Oilfield Company, PetroChina, Tangshan 063000, China; zcy_caoym@petrochina.com.cn
* Correspondence: ych569@126.com

Abstract: CO_2 displacement is an important technology to reduce emissions and improve crude oil recovery, as well as prevent CO_2 escape. Effective storage is key to the successful implementation of this technology, especially for medium and high permeability reservoirs. The current flow control systems that are applied to seal gas escape are mainly gas/water alternation, CO_2 foam, and CO_2 foam gel, but there is no clear understanding of the plugging limits of various flow control systems and the mechanism of their combined use of residual oil. Therefore, in this paper, a series of core replacement experiments are conducted for different flow control systems and their combinations. The quantitative characterization of the core pore size distribution before and after the replacement is carried out using the NMR technique to try and determine the plugging limits of different plugging systems, and to investigate the residual oil utilization patterns of self-designed flow control system combinations and common flow control system combinations under two reservoir conditions with and without large pores. The results show that the plugging limits of water/gas alternation, CO_2 foam, and CO_2 foam gel systems are 0.86–21.35 μm, 0.07–28.23 μm, and 7–100 μm, respectively, as inferred from the T_2 (lateral relaxation time) distribution and pore size distribution. When different combinations of flow control systems are used for repelling, for reservoirs without large pore channels, the combination of flow control systems using higher strength CO_2 foam first can effectively improve the degree of crude oil mobilization in small pore throats, compared to using gas/water alternation directly. For reservoirs containing large pore channels, using high-strength CO_2 foam gel first to seal the large pore channels increases the degree of utilization of the large pore channels; using water/gas alternation first causes damage to the middle pore channels; High-strength CO_2 foam gel seals the large pore channels when the plugging strength is not enough; and using water/gas alternation can effectively improve the degree of utilization of small and medium pore channels. The results of this paper can provide theoretical guidance for the multi-stage flow control of CO_2 displacement in the field.

Keywords: CO_2 displacement seal gas escape; nuclear magnetic resonance (NMR); flow control limit systems; segment plug combination; plugging limits

check for updates

Citation: Yang, C.-H.; Lu, P.-P.; Cao, Y.-M.; Xu, M.; Yu, Z.-Y.; Cheng, P.-F. Study on the Plugging Limit and Combination of CO_2 Displacement Flow Control System Based on Nuclear Magnetic Resonance (NMR). *Processes* **2022**, *10*, 1342. https://doi.org/10.3390/pr10071342

Academic Editor: Alfredo Iranzo

Received: 17 June 2022
Accepted: 7 July 2022
Published: 10 July 2022

1. Introduction

In recent years, CO_2 displacement technology has developed rapidly and is another important oil drive technology after water flooding and polymer displacement [1,2]. Compared with water flooding, CO_2 displacement increases the wave volume, has a greater ability to mobilize crude oil in smaller pore roars, can achieve the effective utilization and geological storage of CO_2 (which can be of benefit both economically and environmentally), and has good application prospects [3,4]. However, the non-homogeneity of the reservoir, the viscous finger of gas, and the gravity overburden lead to the problem of gas scattering during CO_2 displacement, which seriously reduces the gas wave efficiency and affects the effect of CO_2 displacement [5–7], especially for the medium and high permeability reservoirs where CO_2 displacement is implemented. Thus, whether the scattering can be effectively sealed is an important issue for the application of CO_2 displacement in the field.

To solve this problem, many scholars have conducted studies that are based on both controlling the flow of injected fluid and plugging the high permeability channels [8–11]. For example, Shen et al. [12] developed an air tampering plugging system for low permeability fractured reservoirs to solve the problems of conventional sealants with difficult injection, poor stability, and poor plugging strength, which is N, N-dimethyl mustard amide tertiary amine (DMETA). PU et al. [13] synthesized novel CO_2-responsive prefabricated gel particles with the interpenetrating network (IPN-ASSAP), which can better achieve gas tampering plugging in tight oil reservoirs with complex fracture networks after hydraulic fracturing. Li et al. [14] formed gels in situ based on a CO_2-sensitive gel system (modified polyacrylamide-methylene-amine-resorcinol gel system), which could better control the gel time. The focus of the above researchers was on how to develop flow control systems with better results, but how to combine flow control systems with more mature processes to improve crude oil recovery seems to be the question of interest for oil producers. Currently, the main flow control systems that are used to seal gas scramble are water/gas alternate injection (WAG), CO_2 foam injection, and CO_2 foam gel injection [15–17]. In mine practice, improper combinations of different flow control systems and mismatches with formation pore throats have caused oil in large pore channels to be squeezed into small pore throats without being driven out [18], and plugging failure affecting the final recovery is reported from time to time. The clarification of the pore roar range of different flow control systems will be the basis for the combination of different flow control systems to improve the recovery of crude oil, while the conventional core drive can only study the effect of different flow control systems to improve the recovery of crude oil from a macroscopic point of view, but cannot reflect its characteristics on microscopic pore plugging and mobilization [19,20].

Therefore, in this paper, we used high-temperature and high-pressure repulsion + nuclear magnetic resonance [21,22], and used non-homogeneous natural cores with simulated formation conditions (temperature: 80 °C, mineralization: 30,000 mg/L) to carry out a study on the plugging limits and combinations of three flow control systems: CO_2 repulsion water/gas alternation, CO_2 foam, and CO_2 foam gel at the nanoscale, in order to determine the microscopic pore throats from cores before and after repulsion. The purpose of this study is to determine the range of different types of flow control systems and their plugging limits from the microscopic pore throat distribution characteristics of the core before and after the repulsion, in order to achieve effective plugging in the process of CO_2 displacement in medium and high permeability reservoirs step by step and avoid "contamination" (subsequent system entry channels or oil flow channels blocked), thus providing theoretical guidance for the multi-stage flow control of CO_2 displacement in the field.

2. Experimental Procedure and Steps

2.1. Experimental Flow

The experiment mainly consists of an NMR instrument, thermostat, foam generator, non-magnetic core holder, ISCO constant speed and constant pressure pump, gas cylinder, intermediate vessel, vacuum pump, pressure gauge, and measuring cylinder. The experimental flow is shown in Figure 1.

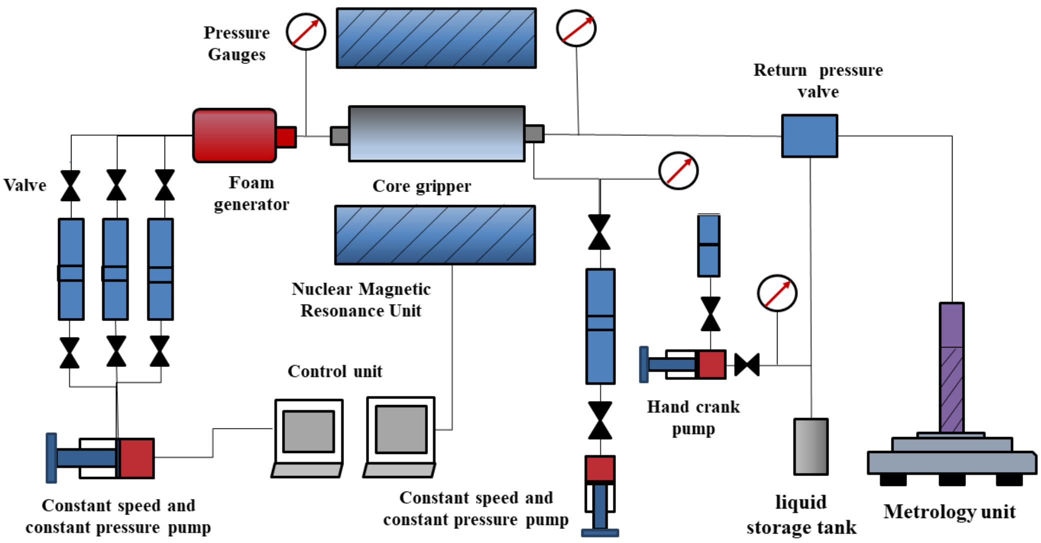

Figure 1. Flow of high temperature and high-pressure online NMR core repulsion experiment.

2.2. Experimental Steps

(1) Core drying. The samples are dried for 24 h at a temperature of 105 °C and then weighed for dry weight. The dry sample is placed into the NMR equipment and tested for dryness. (2) Core saturation with water. The core is vacuumed using a vacuum pump so that the water is pumped into the core and saturation is completed. (3) Core is saturated with oil to establish bound water. After saturating with water, the saturated oil is repelled from one end of the core, and the saturated oil ends, and the water remaining in the core becomes bound water, which is left for some time (aging) to test the T_2 spectrum and nuclear magnetic images in the saturated oil state. (4) Alternating water/gas system plugging. Manganese chloride water and CO_2 are injected alternately to simulate CO_2-water alternate plugging, and the alternation is continued until the T_2 spectrum signal does not change. The T_2 spectrum and NMR images are tested during the experiment. (5) CO_2 foam plugging. Next, 0.6 PV foam (heavy water configuration) and CO_2 are injected into the foam generator at the front of the core, according to the gas–liquid ratio of 1:2. The foam is formed and then injected into the core to simulate CO_2 foam system plugging. It is then repelled until the T_2 spectrum signal does not change. (6) CO_2 foam gel plugging. The 0.6 PV gel and foam mixture with CO_2 are injected into the foam generator at the front of the core, according to the gas–liquid ratio of 1:2, in order to form a CO_2 foam gel system. This is then injected into the core to simulate the plugging of the CO_2 foam gel system and repelled until the T_2 spectrum signal does not change. The T_2 spectrum and NMR images are tested. (7) The changes in oil-repelling efficiency and crude oil utilization in different pore throats are calculated according to the changes in the T_2 spectrum. (8) The T_2 spectra that are measured by the NMR experiments are transformed into pore radius distribution, according to the transformation relationship between relaxation time distribution and pore radius distribution [14,15].

3. Experimental Results and Analysis

3.1. Plugging Boundary

3.1.1. Water/Gas Alternate System Plugging Boundary

Core No. 1 is a medium permeability core with a permeability of 127×10^{-3} μm^2. The NMR T_2 spectra and pore throat radius distribution before and after water/gas alternation in the core are shown in Figures 2 and 3.

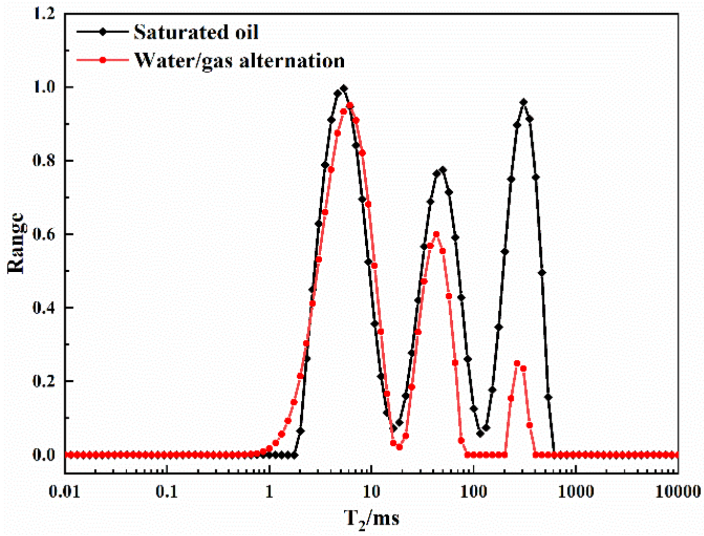

Figure 2. NMR T_2 spectrum of core 1 before and after water/gas alternation.

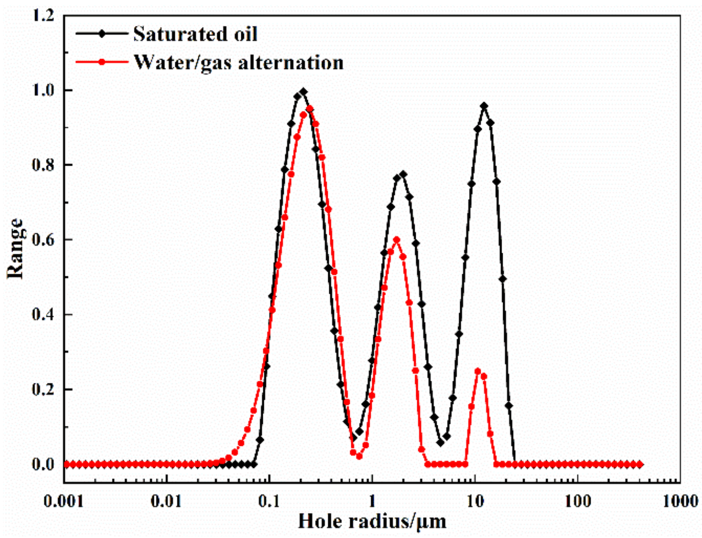

Figure 3. Distribution of pore throat radius before and after water/gas alternation in core No. 1.

From Figure 2, it can be seen that after the water/gas alternating system is carried out in core No. 1, the oil drive efficiency can reach 50.84%, and the high amplitude value area on the T_2 spectrum decreases obviously, indicating that the degree of large pore throat activation is higher during the water/gas alternating process.

From Figure 3, it follows that the remaining oil after the water/gas alternation is mainly distributed in 0.045–0.65 μm and 0.86–3.02 μm pore throats, and a small amount is distributed in 9.24–16.15 μm pore throats. The pore throat activation range is 0.86–4.60 μm and 4.60–21.35 μm; the recovery rate is 0%, 40.9%, 88.2% from the left peak to the right peak, in order; and the water/gas alternating system plugging limit is 0.86–21.35 μm.

3.1.2. CO_2 Foam System Plugging Boundary

After the water/gas alternation in core No. 1 was dried with carbon tetrachloride oil wash, and after saturated water and saturated oil were used to establish bound water, CO_2 foam was injected. The NMR T_2 spectra and pore throat radius distributions before and after CO_2 foam injection are shown in Figures 4 and 5.

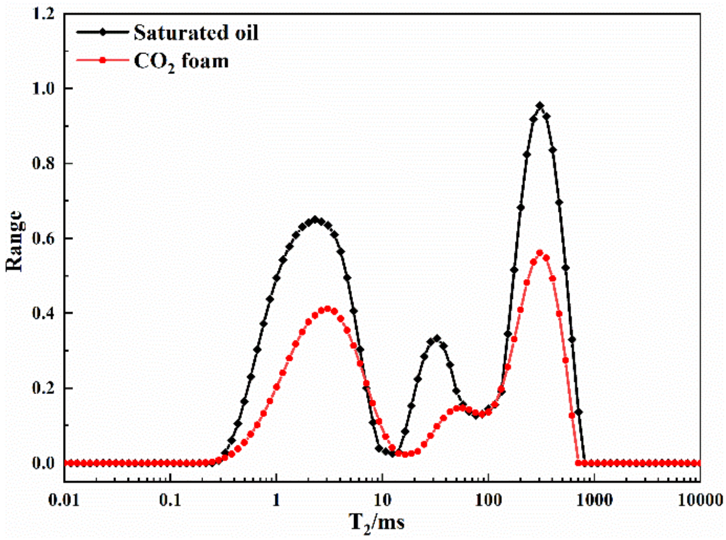

Figure 4. NMR T_2 spectra before and after injection of CO_2 foam in core No. 1.

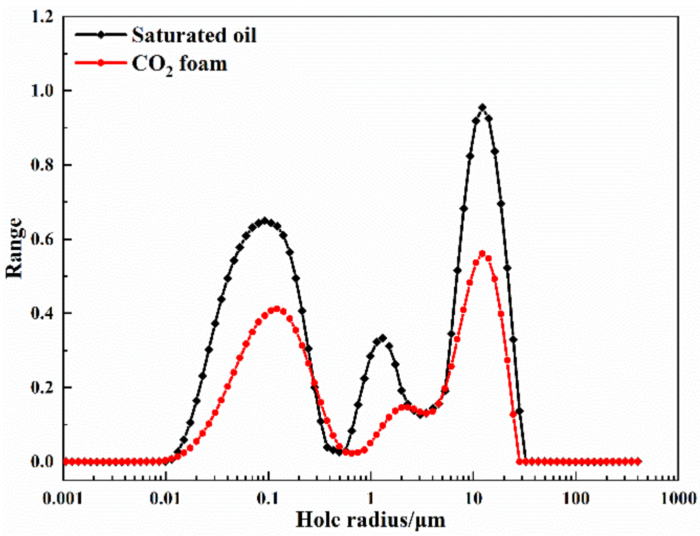

Figure 5. Pore throat radius distribution before and after CO_2 foam injection in core No. 1.

From Figure 4, the oil drive efficiency is 52.76% after the injection of CO_2 foam in core No. 1. Since core No. 1 was saturated several times, the fluid properties in the core changed to some extent, causing the saturated oil amplitude value of the core to become smaller on the T_2 spectrum. The T_2 spectrum shows that the low amplitude value area decreases significantly after the injection of CO_2 foam plugging, indicating a high degree of small pore throat activation.

From Figure 5, it can be seen that after injecting CO_2 foam, the oil mobilization effect in the small pore throat is obvious. The pore throat mobilization range is 0.07–0.49 μm, 0.49–3.02 μm, and 3.02–28.23 μm. The remaining oil is mainly distributed in 0.47–24.54 μm pore throat and partly distributed in 0.015–0.49 μm pore throat. The recoveries are 40.3%, 56.8%, and 39.5% from the left peak to the right peak, in order. The plugging limit of the CO_2 foam system is 0.07–28.23 μm.

3.1.3. CO_2 Foam Gel System Plugging Boundary

To verify the plugging limit of the CO_2 foam gel system, a high permeability No. 2 core with a permeability of 643×10^{-3} μm^2 was selected. The NMR T_2 spectra and pore throat radius distributions before and after the injection of CO_2 foam gel are shown in Figures 6 and 7.

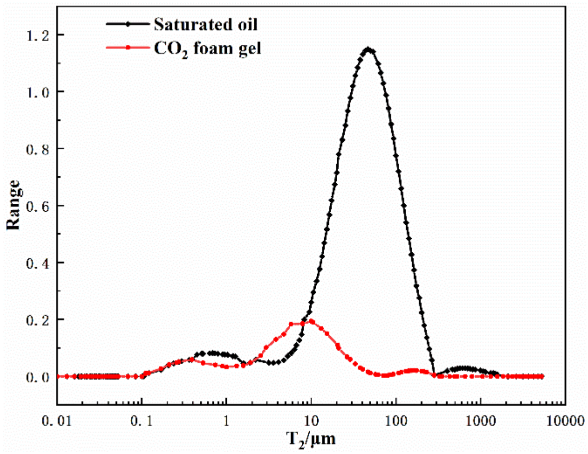

Figure 6. NMR T_2 spectra of core No. 2 before and after injection of CO_2 foam gel.

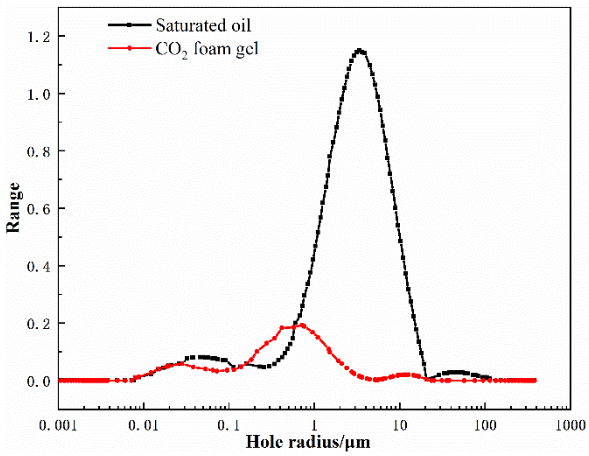

Figure 7. Pore throat radius distribution before and after injection of CO_2 foam gel in core No. 2.

From Figure 6, it can be seen that after injecting CO_2 foam gel in core No. 2, the oil repelling efficiency is 89.2%, and the high amplitude value area on the T_2 spectrum decreases obviously, indicating that the large pore channel is effectively used; the low amplitude value area on the T_2 spectrum increases, indicating that some crude oil is squeezed into the small pore throat when CO_2 foam gel plugging is performed.

From Figure 7, it can be seen that the large pore throats in the CO_2 foam gel plugging stage are basically all used, the pore throats are used in the range of 7–100 μm, and the remaining oil is mainly distributed in the 0.084–3.12 μm pore throats. The recovery rate is 95.1%, almost all of which is concentrated in the large pore channel, and the plugging limit of the CO_2 foam gel system is 7–100 μm.

3.2. *Different Combinations of Flow Control Systems*

According to the field practice and plugging intensity, the usual combination of flow control for CO_2 displacement is water/gas alternation + CO_2 foam or CO_2 foam gel (after gas firing) + water/gas alternation; however, whether this combination is reasonable and can maximize the utilization of oil remaining in different pore throats needs further verification. In this study, a high-temperature and high-pressure online NMR system was used to seal the pore with high-strength CO_2 foam or CO_2 foam gel before water/gas alternation, then compared with the conventional combination to study the degree of pore throat utilization and the ability to improve crude oil recovery, in order to select different combinations of flow control systems and provide a construction basis for on-site CO_2 displacement plugging.

3.2.1. Combination of Different Flow Control Systems for CO_2 Displacement in Reservoirs without Large Pores

Since there is no large orifice, the CO_2 foam gel plugging system is not considered and is sealed with a combination of alternating water/gas system and a higher strength plugging CO_2 foam system.

(1) Water/gas alternation + CO_2 foam + water/gas alternation

The permeability of core No. 3 is 194 × 10^{-3} μm^2, and the NMR T_2 spectra and pore throat radius distributions of the cores with different flow control systems are shown in Figures 8 and 9.

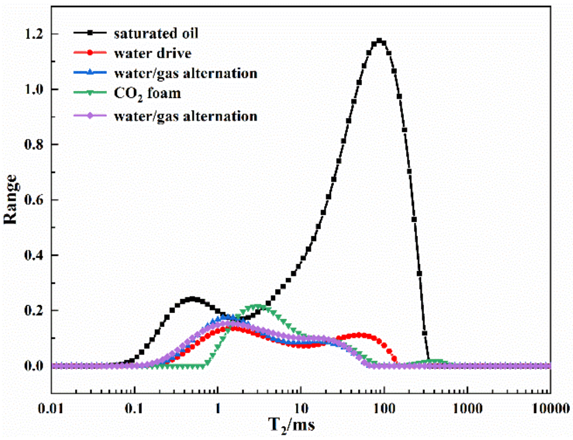

Figure 8. NMR T_2 spectra of different flow control systems in core No. 3.

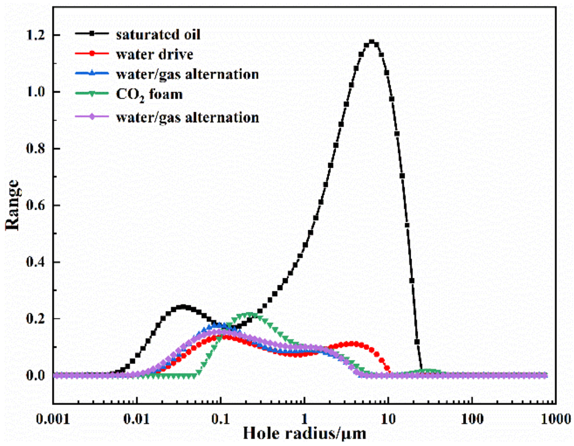

Figure 9. Pore throat radius distribution of different flow control systems in core No. 3.

From Figures 8 and 9, the oil content in the large pore throat decreased significantly after the water drive, and the range of pore throat utilization was 0.39–22.12 μm. The oil drive efficiency in the water drive stage was 49.62%, and the high amplitude value of the T_2 spectrum decreased significantly, mainly because the oil in the large pore throat was driven out. After the water/gas alternation, the oil in the large pore throat decreased, the range of pore throat utilization was 2.06–9.57 μm, and the oil drive efficiency increased by 11.81%. After the low plugging strength led to gas escape, the pore throat was blocked with a higher strength CO_2 foam, the range of pore throat motility was 0.02–0.14 μm, and the oil drive efficiency increased by 13%. The T_2 spectrum decreased significantly in the low amplitude value region, indicating that the oil in the small pore throat was driven out. After that, the water/gas alternation was performed again, and the increase in oil drive efficiency was very small, only 1.18%. The oil in the pore throat was not significantly reduced, and the pore throat was poorly used. The combination improved the recovery rate by 75.61% overall.

(2) CO_2 foam + water/gas alternation + CO_2 foam + water/gas alternation

The permeability of core No. 4 is 199 × 10^{-3} μm^2, and the NMR T_2 spectra and pore throat radius distributions of the cores with different flow control systems are shown in Figures 10 and 11.

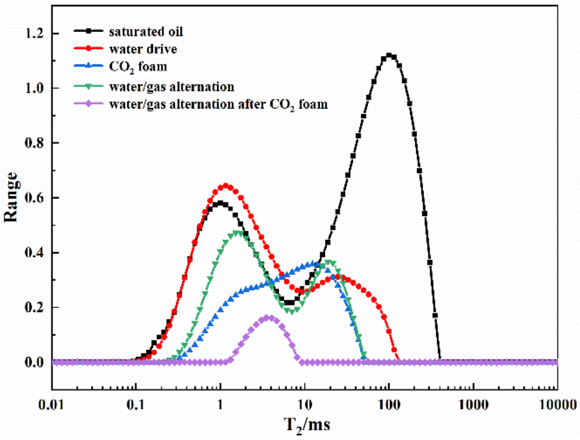

Figure 10. NMR T_2 spectra of different flow control systems in core No. 4.

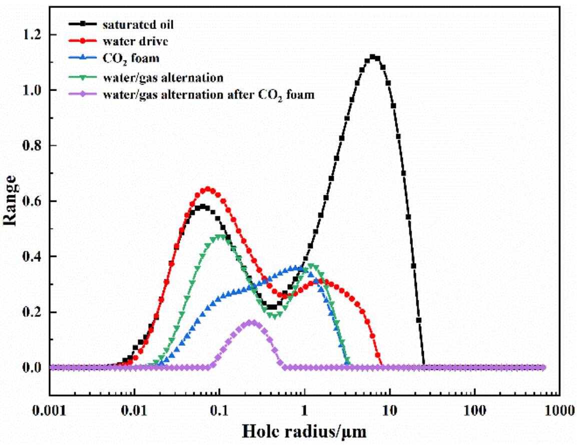

Figure 11. Pore throat radius distribution of different flow control systems in core No. 4.

From Figures 10 and 11, the oil content in the large pore throat decreases significantly after the water drive, the pore throat mobilization range is 0.89–25.47 μm, the oil drive efficiency in the water drive stage is 57.26%, the large pore throat is mobilized to a high degree, and the small pore throat is not mobilized. At the end of the water drive, a higher strength CO_2 foam plugging is injected, the oil in the small pore throat decreases significantly, the pore throat dynamic range is from 0.012 to 0.77 μm and 1.56 to 7.25 μm, and the oil drive efficiency is increased by 6.36%. After the water/gas alternation, the CO_2 is shifted and it is easier to use the crude oil in the small pore throat, and the crude oil in the small pore throat is mainly replaced. After alternating water/gas injection, the pore throat activation range is 0.023–0.22 μm and 1.01–1.79 μm, the oil repelling efficiency increases by 25.45%, and the T_2 spectrum decreases significantly in the low amplitude area, reflecting the higher degree of activation of smaller pore throats. Finally, after CO_2 foam plugging + alternating water/gas, the pore throat activation range is 0.02–3.14 μm, and the oil repelling efficiency increases by 5.53%; both smaller and larger pore throats are used, and the oil repelling effect is good. The combination increases the recovery rate by 94.6% overall.

Comparing Figures 9 and 11, when developing reservoirs without large orifices, the smaller orifices are used to a higher degree when the higher-strength CO_2 foam plugging is performed first, followed by water/gas alternation, and the smaller orifices are used to a higher degree when the plugging strength is not enough to cause gas escape.

3.2.2. Combination of Different Flow Control Systems for CO_2 Displacement in Reservoirs Containing Large Pore Channels

Since it contains large orifices, a combination of alternating water/gas systems and a high-strength CO_2 foam gel plugging system is considered for plugging.

(1) Water/gas alternation + CO_2 foam gel + water/gas alternation

The permeability of core No. 5 is 643×10^{-3} μm^2, and the NMR T_2 spectra and pore throat radius distribution of the cores with different flow control systems are shown in Figures 12 and 13.

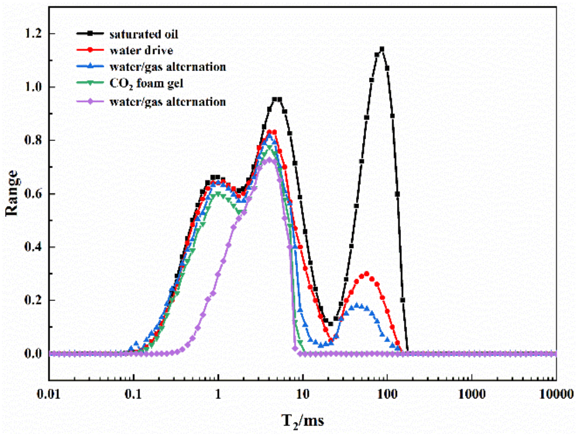

Figure 12. NMR T_2 spectra of different flow control systems in core No. 5.

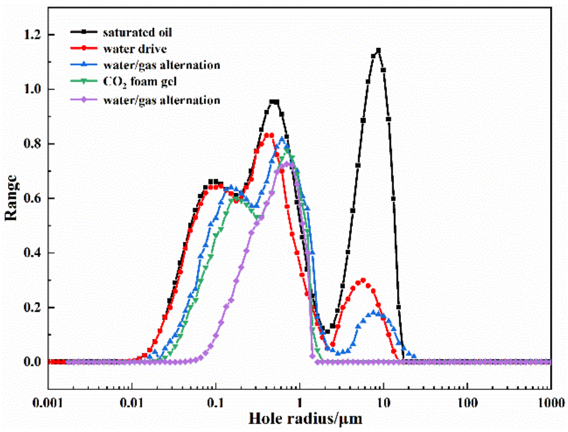

Figure 13. Pore throat radius distribution of different flow control systems in core No. 5.

From Figures 12 and 13, the pore throat activation range in the core water drive stage is 0.15–5.02 μm, and the oil drive efficiency is 34%. After alternate water/gas injection, the pore throat activation range is 1.64–5.02 μm, and the oil drive efficiency increases by 8.5%. The T_2 spectrum decreases significantly in the high amplitude value area, and the degree of large pore throat activation is high. Once the seal strength is low, which leads to gas fugacity, the high strength CO_2 foam gel is used to seal the large pore channel, and the pore throat activation range is small, mainly in the range of 0.31–0.54 μm; the oil drive efficiency is increased by 9.7%, and the T_2 spectrum shows that the medium pore throat activation is better. Then, the water/gas alternation is carried out, and the small pore throat activation is obvious; the activation range is 0.006–0.066 μm, and the oil drive efficiency is increased significantly by 15.8%. The combination increases the recovery rate by 68% overall, and the T_2 spectrum shows good activation of the small pore throat, indicating that the CO_2 foam gel plugging plays a role in plugging the large pore channel.

(2) CO_2 foam gel + water/gas alternation + CO_2 foam gel + water/gas alternation

The permeability of core No. 6 is 639 × 10^{-3} μm^2, and the NMR T_2 spectra and pore throat radius distribution of the cores with different flow control systems are shown in Figures 14 and 15.

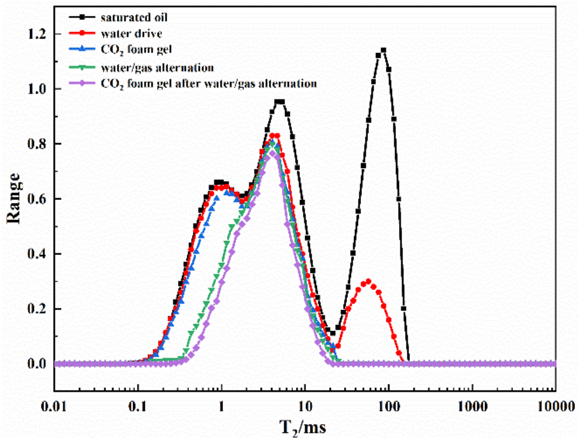

Figure 14. NMR T_2 spectra of different flow control systems in core No. 6.

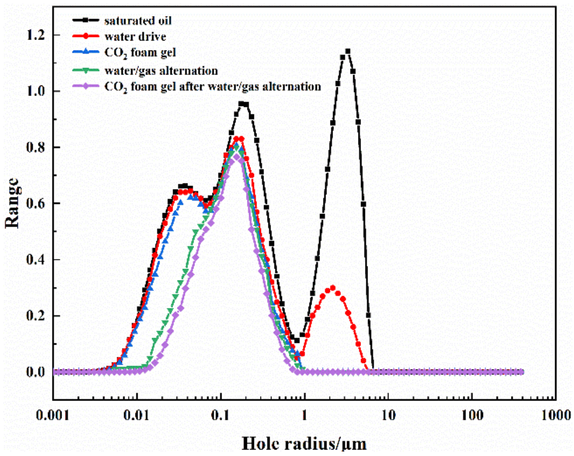

Figure 15. Pore throat radius distribution of different flow control systems in core No. 6.

From Figures 14 and 15, it can be seen that the pore throat activation range of the core water drive stage is from 0.11 to 5.77 μm, the oil drive efficiency is 36%, the T_2 spectrum high amplitude value area decreases obviously, the degree of large pore throat activation is high, and the small pore throat is basically not activated. The water drive ends with high strength CO_2 foam gel to seal the large pore channel; all the oil in the large pore throat is activated, the small pore throat is partially activated, the pore throat activation range is 0.012–0.77 μm and 0.94–5.77 μm, and the oil drive efficiency increases by 14.82%. Then, the water/gas alternation is carried out. The pore throat is used in the range of 0.006–0.07 μm, and the oil drive efficiency increases by 6.14%, while the T_2 spectrum decreases significantly in the low amplitude area, reflecting the higher use of smaller pore throats. Finally, CO_2 foam gel plugging + water/gas alternate plugging is performed, and the medium pore throat is basically not used; he improvement of the oil drive efficiency is only 0.82%. The overall recovery improvement is only 57.8%.

Comparing Figures 13 and 15, when developing reservoirs containing large pore channels, water/gas alternation is performed first to move small and medium pore throats, and after gas escape that is caused by low strength, high strength CO_2 foam gel plugging + water/gas alternation is performed with a high degree of pore throat movement and good oil drive effect.

3.3. Discussion of Results

The high-temperature and high-pressure repulsion + NMR method is an effective means by which to study the plugging limits and combination characteristics that are adapted to different flow control systems of CO_2 displacement at the microscopic nanoscale. The NMR T_2 spectra and pore throat radius distribution trends reflect the fluid distribution in the pore space of different cores. The variation of the magnitude values characterize the utilization of crude oil in the pore space and the remaining oil range after the injection of different flow control systems, and determine the minimum and maximum pore throats that are entered by different flow control systems, from which the plugging limits can be inferred. The experimental results show that the alternating water/gas system uses a minimum pore throat radius of 0.86 μm, a maximum pore throat radius of 21.35 μm, and a plugging limit of 0.86–21.35 μm. The CO_2 foam system uses a minimum pore throat radius of 0.07 μm and a maximum pore throat radius of 28.23 μm, with a plugging limit of 0.07–28.23 μm. The minimum pore throat radius of the CO_2 foam gel system is 7 μm, the maximum pore throat radius is 100 μm, and the plugging limit is from 7 to 100 μm. Compared with the alternating water/gas system, the CO_2 foam system has a higher plugging strength, a larger range of accessible pore throats, the ability to use the crude oil in the small pore roar, and a lower limit of the used pore throat radius reaching 0.07 μm. The CO_2 foam gel system is a high viscosity system with the highest plugging strength, mainly for plugging large pores, and the upper limit of plugging pore roar reaches 100 μm. The upper limit of the plugging of three flow control systems, namely water/gas alternate, CO_2 foam, and CO_2 foam gel, becomes larger in turn, and the plugging strength is enhanced step by step.

In practice, medium and high permeability reservoirs have large pore throats and strong non-homogeneity, so the plugging strength of the plugging agent is required to be high when plugging fractures with large openness and large pore throats. The plugging agent is required to have a good injection performance when plugging small and medium pores in the matrix. Single water-air alternating system and foam system have good injection performance, but the plugging strength is limited and cannot achieve the effective mobilization of crude oil in low permeability areas. A single gel plugging system with high strength can plug large pore channels such as fractures, but it cannot achieve complete plugging due to the existence of the marginal effect. Therefore, in my practice, a combination of three plugging systems is often used to improve the effectiveness of the gas drive. Usually, the flow control combination of CO_2 displacement is water/gas alternation + CO_2 foam or CO_2 foam gel (carried out after gas scramble) + water-gas alternation; however, whether this combination is reasonable and whether it can maximize the use of oil remaining in different pore throats needs further verification. Therefore, based on the study of the plugging limit, experiments are conducted to investigate the law of using the remaining oil in different combinations of flow control systems for two types of reservoirs with and without large orifices. Compared with foam systems, most gels are high-viscosity systems with higher plugging strength and are often used to plug large seepage channels, so the combination of CO_2 foam gel plugging systems is not considered in the study of plugging combinations without large pores. The combination of an alternating water/gas system and a high-strength CO_2 foam gel plugging system was used for plugging with large pores. The results show that for reservoirs without large pores, firstly, with high strength CO_2 foam plugging, then water/gas alternation, CO_2 can easily turn into smaller pore throats to achieve the effective repulsion of crude oil in small pore throats; with high strength CO_2 foam blocking + water/gas alternation when the plugging strength is not enough to cause gas escape, both large and small pore throats can be used to improve the recovery of crude oil, and the repelling effect is good. For reservoirs containing large pore channels, high-strength CO_2 foam gel plugging is used first. Although the large pore channels are better used, they also contaminate the middle pore throats, resulting in the subsequent replacement of the middle pore throats that cannot be used, which affects the final recovery of crude oil. Therefore, when developing reservoirs containing large pores, firstly, water/gas alternation is carried out to activate small and medium pore throats.

After the gas firing, high-strength CO_2 foam gel blocking + water/gas alternation is carried out. The combination of the high degree of pore throat activation leads to the overall improvement of crude oil recovery, and good oil drive effect.

4. Conclusions

In this paper, the plugging limits of three flow control systems, namely water/gas alternation, CO_2 foam, and CO_2 foam gel, are quantified through high temperature and high-pressure repulsion + NMR, and the degree of residual oil mobilization by different combinations of flow control systems is further investigated. The experimental results show that the plugging limit of an alternating water/gas system is 1.51–21.35 μm; the plugging limit of a CO_2 foam system is 0.07–28.23 μm. The plugging limit of the CO_2 foam gel system is 7–100 μm. The CO_2 foam system has the strongest ability to use small pore throat, and the lower limit of pore throat can be used up to 0.07 μm. The CO_2 foam gel system is a high-viscosity system with the highest sealing strength, which is mainly suitable for plugging large orifices. For reservoirs without large pore channels, the first higher strength CO_2 foam plugging, followed by alternate low strength water/air plugging, makes it easy for CO_2 to shift into smaller pore throats, improves the degree of use of small pore throats, and has the best overall oil drive effect. For reservoirs containing large pore channels, firstly, alternate water/air plugging, and then use CO_2 foam gel when the plugging strength is not enough, which can avoid the contamination of the gel to the middle hole, improve the degree of use of the small and middle hole throat, and produce a good oil repelling effect. In addition, the experimental results of core replacement with different combinations of flow control systems show that the injection sequence of various flow control systems has an obvious effect on the final recovery rate, and the injection timing and injection parameters of various plugging systems need to be further studied to avoid harming the reservoir properties. The experimental conclusion provides theoretical guidance for the multi-stage flow control of CO_2 displacement in the field.

Author Contributions: Conceptualization, C.-H.Y.; methodology, validation, resources, data curation, and writing—original draft writing preparation, P.-P.L., M.X., Z.-Y.Y. and P.-F.C.; writing—review and editing, visualization, and supervision, Y.-M.C. and C.-H.Y.; project administration, C.-H.Y. All authors have read and agreed to the published version of the manuscript.

Funding: This study is supported by the bureau-level key research project "Research on the leading technology and application of gas drive in shallow and medium-deep high water-bearing reservoirs (JDYT-2019-JS-262)".

Institutional Review Board Statement: Not applicable.

Informed Consent Statement: Not applicable.

Data Availability Statement: Not applicable.

Conflicts of Interest: None of the authors of this paper has a financial or personal relationship with other people or organizations.

References

1. Han, J.; Han, S.; Sung, W.; Lee, Y. Effects of CO_2 miscible flooding on oil recovery and the alteration of rock properties in a carbonate reservoir. *J. CO_2 Util.* **2018**, *28*, 6–40. [CrossRef]
2. Wang, Q.; Yang, S.; Han, H.; Wang, L.; Qian, K.; Pang, J. Experimental Investigation on the Effects of CO_2 Displacement Methods on Petro physical Property Changes of Ultra-Low Permeability Sandstone Reservoirs Near Injection Wells. *Energies* **2019**, *12*, 327. [CrossRef]
3. Zhang, T.; Tang, M.; Ma, Y.; Zhu, G.; Zhang, Q.; Wu, J.; Xie, Z. Experimental study on CO_2/Water flooding mechanism and oil recovery in ultralow-Permeability sandstone with online LF-NMR. *Energy* **2022**, *252*, 123948. [CrossRef]
4. Liu, S.Y.; Ren, B.; Li, H.Y.; Yang, Y.-Z.; Wang, Z.-Q.; Wang, B.; Xu, J.-C.; Agarwal, R. CO_2 storage with enhanced gas recovery (CSEGR): A review of experimental and numerical studies. *Pet. Sci.* 2021, *in press*. [CrossRef]
5. Tian, W.; Li, P.; Lu, Z.; Lu, D. Experimental investigation and numerical simulation of viscous fingering in porous media during CO_2 flooding. *J. Porous Media* **2019**, *229*, 1493–1506. [CrossRef]

6. Luo, J.; Hou, Z.; Feng, G.; Liao, J.; Haris, M.; Xiong, Y. Effect of Reservoir Heterogeneity on CO_2 Flooding in Tight Oil Reservoirs. *Energies* **2022**, *15*, 3015. [CrossRef]
7. Li, J.; Chuanzhi, C.; Wu, Z.; Wang, Z.; Yang, H. Study on the Migration Law of CO_2 Miscible Flooding Front and the Quantitative Identification and Characterization of Gas Channeling. *SSRN* **2022**. [CrossRef]
8. Zhao, F.; Wang, P.; Huang, S.; Hao, H.; Zhang, M.; Lu, G. Performance and applicable limits of multi-stage gas channeling control system for CO_2 flooding in ultra-low permeability reservoirs. *J. Pet. Sci. Eng.* **2020**, *192*, 107336. [CrossRef]
9. Wang, C.; Ma, B.; Zhang, L. Experimental study on CO_2 capture by using n-butylamine to plug the gas channeling to enhanced oil recovery. *J. Pet. Explor. Prod. Technol.* **2022**, 1–9. [CrossRef]
10. Du, L.; Lu, T.; Li, B. CO_2 capture and sequestration in porous media with SiO_2 aerogel nanoparticle-stabilized foams. *Fuel* **2022**, *324*, 124661. [CrossRef]
11. Du, Q.; Hou, J.; Zhao, F.; Zhou, K.; Liu, W.; Liu, Y. A new organic fiber composite gel as a plugging agent for assisting CO_2 huff and puff in water channeling reservoirs. *J. Pet. Sci. Eng.* **2019**, *179*, 70–79. [CrossRef]
12. Shen, H.; Yang, Z.; Li, X.; Peng, Y.; Lin, M.; Zhang, J.; Dong, Z. CO_2-responsive agent for restraining gas channeling during CO_2 flooding in low permeability reservoirs. *Fuel* **2021**, *292*, 120306. [CrossRef]
13. Pu, W.; Du, D.; Fan, H.; Chen, B.-W.; Yuan, C.-D.; Varfolomeev, M.A. CO_2-responsive preformed gel particles with interpenetrating networks for controlling CO_2 breakthrough in tight reservoirs. *Colloids Surf. A Physicochem. Eng. Asp.* **2021**, *613*, 126065. [CrossRef]
14. Li, D.X.; Zhang, L.; Liu, Y.M.; Kang, W.-L.; Ren, S.-R. CO_2-triggered gelation for mobility control and channeling blocking during CO_2 flooding processes. *Pet. Sci.* **2016**, *13*, 247–258. [CrossRef]
15. Kong, D.; Gao, Y.; Sarma, H.; Li, Y.; Guo, H.; Zhu, W. Experimental investigation of immiscible water-alternating-gas injection in ultra-high water-cut stage reservoir. *Adv. Geo-Energy Res.* **2021**, *5*, 139–152. [CrossRef]
16. Kang, W.; Jiang, H.; Yang, H.; Li, Z.; Zhou, B.; He, Y.; Sarsenbekuly, B.; Gabdullin, M. Study of nano-SiO_2 reinforced CO_2 foam for anti-gas channeling with a high temperature and high salinity reservoir. *J. Ind. Eng. Chem.* **2021**, *97*, 506–514. [CrossRef]
17. Xu, T.; Wei, Y.; Ma, T. Experiment and Simulation of Gas Channeling Control Technique During CO_2 Flooding in Normal Pressure Tight Oil Reservoir of South Ordos Basin. Abu Dhabi International Petroleum Exhibition & Conference. *One Petro* **2020**. [CrossRef]
18. Ding, S.; Wang, L.; Li, M.; Zhao, C.; Han, B.; Song, Z.; Xu, L.; Liu, Q.; Hou, J.; Song, L. Study on Control Technology of Carbon Dioxide Flooding Gas Channeling in Low Permeability Reservoir. In Proceedings of the International Field Exploration and Development Conference, Chengdu, China, 23–25 September 2020; Springer: Singapore, 2020; pp. 2786–2794. [CrossRef]
19. Li, Y.; Yao, Y.; Qi, M.; Zhao, C.; Han, B.; Song, Z.; Xu, L.; Liu, Q.; Hou, J.; Song, L. Experimental Modeling of Gas Channeling for Water-alternating-gas flooding in High-temperature and High-pressure Reservoirs. In Proceedings of the Carbon Management Technology Conference, Houston, TX, USA, 15–18 July 2019. [CrossRef]
20. Sun, Y.; Li, Q.; Fan, C. Laboratory core flooding experiments in reservoir sandstone under different sequestration pressures using multichannel fiber Bragg grating sensor arrays. *Int. J. Greenh. Gas Control.* **2017**, *60*, 186–198. [CrossRef]
21. Wei, B.; Liu, J.; Zhang, X.; Xiang, H.; Zou, P.; Cao, J.; Bai, M. Nuclear Magnetic Resonance (NMR) mapping of remaining oil distribution during sequential rate water flooding processes for improving oil recovery. *J. Pet. Sci. Eng.* **2020**, *190*, 107102. [CrossRef]
22. Chen, M.; Dai, J.; Liu, X.; Kuang, Y.; Wang, Z.; Gou, S.; Qin, M.; Li, M. Effect of displacement rates on fluid distributions and dynamics during water flooding in tight oil sandstone cores from nuclear magnetic resonance (NMR). *J. Pet. Sci. Eng.* **2020**, *184*, 106588. [CrossRef]